

S.K. SUNDARAM^{1,✉}
C.B. SCHAFFER²
E. MAZUR³

Microexplosions in tellurite glasses

¹ Environmental Technology Division, Pacific Northwest National Laboratory, Richland, WA 993522, USA

² Department of Chemistry and Biochemistry, University of California, San Diego, CA 92093, USA

³ Division of Engineering and Applied Sciences and Department of Physics, Harvard University, Cambridge, MA 02138, USA

Received: 27 December 2001/Accepted: 9 July 2002
Published online: 25 October 2002 • © Springer-Verlag 2002

ABSTRACT Femtosecond laser pulses were used to produce localized damage in the bulk and near the surface of baseline, Al₂O₃-doped and La₂O₃-doped sodium tellurite glasses. Single or multiple laser pulses were non-linearly absorbed in the focal volume by the glass, leading to permanent changes in the material in the focal volume. These changes were caused by an explosive expansion of the ionized material in the focal volume into the surrounding material, i.e. a microexplosion. The writing of simple structures (periodic array of voxels, as well as lines) was demonstrated. The regions of microexplosion and writing were subsequently characterized using scanning electron microscopy (SEM), energy-dispersive spectrometry (EDS) and atomic force microscopy (AFM). Fingerprints of microexplosions (concentric lines within the region and a concentric ring outside the region), due to the shock wave generated during microexplosions, were evident. In the case of the baseline glass, no chemistry change was observed within the region of the microexplosion. However, Al₂O₃-doped and La₂O₃-doped glasses showed depletion of the dopant from the edge to the center of the region of the microexplosions, indicating a chemistry gradient within the regions. Interrogation of the bulk- and laser-treated regions using micro-Raman spectroscopy revealed no structural change due to the microexplosions and writing within these glasses.

PACS 61.80.Ba; 68.37.Hk; 68.37.Ps; 61.43.Fs

1 Introduction

Tellurite glasses have low melting points, high densities and low transformation temperatures [1, 2]. These glasses are not hygroscopic, making them useful for practical applications. Tellurite glasses have large refractive indices, and, hence, high dielectric constants, and are good IR transmitters for wavelengths up to 5 μm. Tellurite glasses are promising optical materials for use in such products as broadband amplifiers because of low phonon energies and a large third-order non-linear susceptibility [3, 4]. El-Mallawany [5, 6] has recently reviewed the elastic and thermal properties and interpreted the structural aspects of tellurite glasses [7]. In the (Na₂O)_x–(TeO₂)_{1–x} system, the modifier Na₂O can be used to change the Te–O–Te coordina-

tion and thus the glass transition temperature [8, 9] and non-linear optical response [10]. The structural changes in tellurite glasses, due to chemical modification, have been the subject of several studies [11–15]. McLaughlin and coworkers [16] have combined sodium-23 nuclear magnetic resonance (NMR), neutron diffraction, and X-ray diffraction to study and present models of sodium tellurite glasses.

The writing of various optical structures in different materials (for example, Si, SiO₂, SiC, glasses) using femtosecond laser pulses has been demonstrated [17–33]. In these experiments, a femtosecond laser pulse is tightly focused into the bulk of a transparent material. At the focus, the laser intensity can become high enough to induce non-linear absorption of laser energy by the material (multiphoton, tunneling, and avalanche ionization all play a role), resulting in optical breakdown and the formation of a high-density, highly excited plasma. This hot plasma explosively expands into the surrounding material, creating a microexplosion. The result is a permanently damaged region in the bulk of the material. Glezer and co-workers described the size of the voxels, the self-focusing effects, and the material response under conditions of microexplosions in fused silica [18–21]. The damage was found to be confined to a small volume of about 200 nm in diameter and about 1 μm in length. Material left at the center of the microexplosion was either amorphous/less dense or entirely absent. The intensity threshold for breakdown and structural change is typically a few times 10¹³ W/cm² and is only weakly dependent on material properties [23–28]. This paper reports on microexplosions and microstructuring and their impact on the chemistry and structure of tellurite glasses.

2 Experimental

Baseline glasses of composition 10Na₂O–90TeO₂ (mol%) and doped (2 mol% addition of La₂O₃ or 1 mol% addition of Al₂O₃) were used for the present study. La₂O₃ doping was used for its application in laser materials. Al₂O₃ doping was considered as this modifies the Te–O–Te coordination, which was expected to enhance mechanical properties. All glasses were prepared in a batch size of 10 g using reagent-grade chemicals TeO₂ (99.999% pure), Na₂CO₃, La₂O₃, and Al₂O₃. All glasses were melted at 750–800 °C for 30–60 min in air and cooled in air. A new Pt crucible was covered tightly with a Pt lid for each melt. No crystals were detectable in any of the glasses under optical microscopy. The top and bottom surfaces of the glasses were prepared by grinding and

✉ +1-509/376-3108, E-mail: sk.sundaram@pnl.gov

polishing for femtosecond laser writing and microexplosion experiments.

The microexplosions experiments were performed with a Kerr lens-mode-locked, regeneratively amplified Ti:sapphire laser operating at 1 kHz. Chirped-pulse amplification was used to avoid non-linear optical effects in the amplifier. A 140-fs, 800-nm laser pulse was tightly focused inside the bulk of the sample by a microscope objective with a numerical aperture (NA) of 0.45. The sample was moved by a computer-controlled stage and single and multiple laser pulses (shots) were fired into the sample to produce arrays and structures. The energy used for writing varied between 130 nJ and 1.3 μ J. The breakdown threshold was determined to be 15 nJ.

The structures were characterized using optical microscopy, scanning electron microscopy (SEM, JEOL model No. JSM-5900LV), energy dispersive spectrometer (EDS, OXFORD model No. INCA) and atomic force microscopy (Veeco (formerly Digital Instruments) Nanoscope III AFM, with a standard SiN probe tip). The samples were metallographically (grinding and polishing) prepared before the

writing experiments. No preparation was done after the writing. The size, depth of penetration and interaction volume of the electron beams allowed imaging and characterization of the structures written tens of microns beneath the surface. All SEM images were taken using the back-scattered electron mode. Micro-Raman spectroscopy (Spex (Edison, NJ) model 1877 triple spectrometer with model 1482ET Micramate Raman microscope), a micro-sample illuminator and a Princeton Instruments (Trenton, NJ) LN/CCD detector) were used to determine the structural changes due to the microexplosions. Spectral analysis was performed using Princeton Instruments WinSpec and Galactic Industries (Salem, NH) Grams 32/AI software.

3 Results and discussion

3.1 Baseline glass (10Na₂O-90TeO₂)

Figure 1a shows the single-shot damage in the baseline composition glass. In Fig. 1a, the laser energy increases from top to bottom, with laser energies of 130, 205, 325, 520

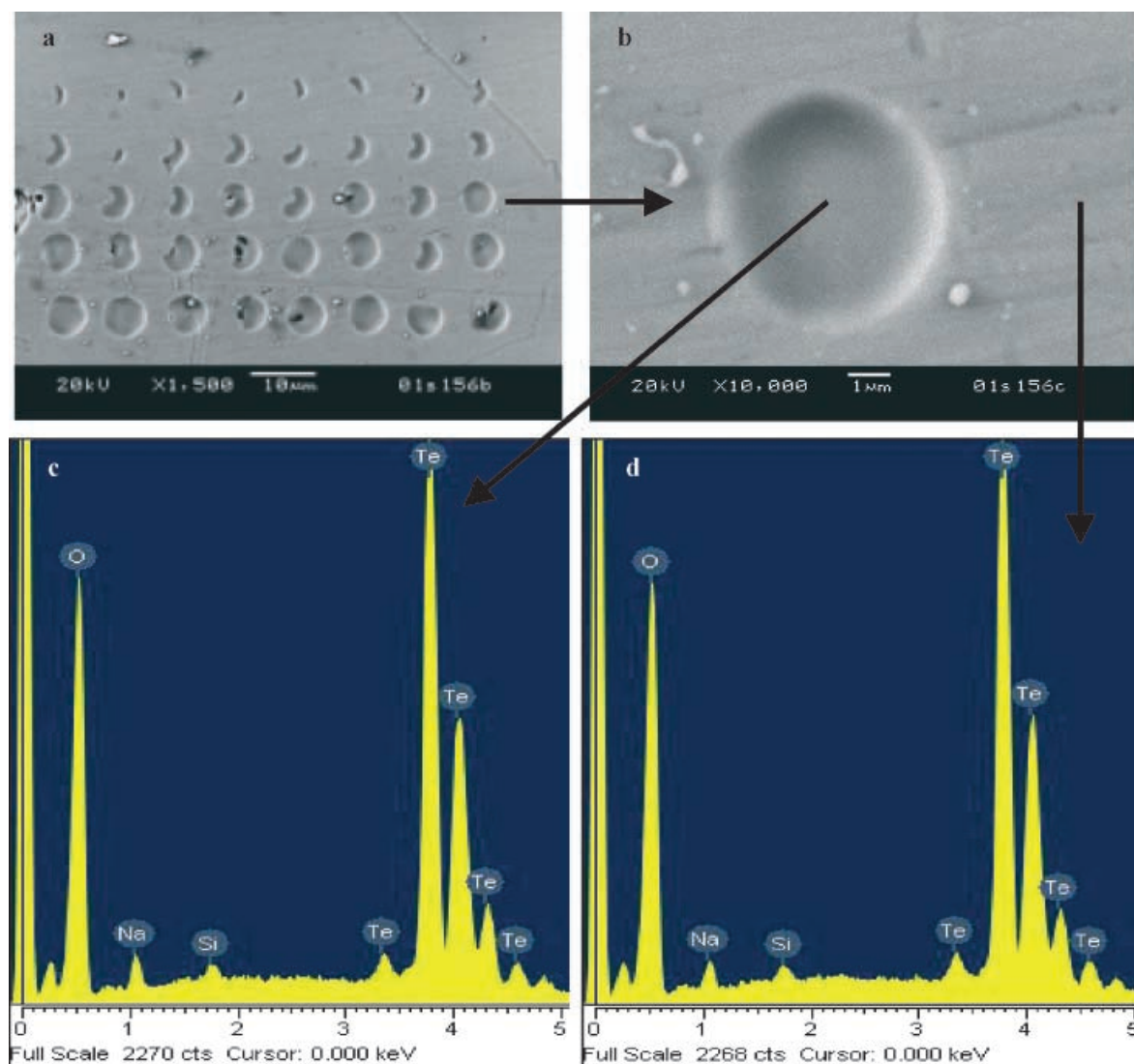


FIGURE 1 SEM images **a** and **b** and EDS data **c** and **d** of the microstructured glass sample. In **a**, the laser energy increases from *top to bottom*, with laser energies of 130, 205, 325, 520, and 820 nJ for successive rows, going from *top to bottom*

and 820 nJ for successive rows, going from top to bottom. The gradual formation of voxels, from half-moon shaped to full circle, was observed. The voxels were spaced with an approximately 10 μm gap. A closer view of one of the circular voxels is shown in Fig. 1b. The point EDS spectra taken inside and outside the voxel are shown in Fig. 1c and d, respectively. The spectra indicated no significant change in the chemistry between the inside and outside the voxel, suggesting a possible physical change (for example, less dense glass) supported by

the contrast in back-scattered-electron SEM images, rather than chemical change due to the microexplosions.

The sample in the as-written state was used for AFM measurements. No sectioning or surface preparation was carried out. The images and data correspond to near-surface features. Figure 2 shows the AFM images of (Fig. 2a) isometric and (Fig. 2b) plan views of one of the circular voxels. Sectional analysis (Fig. 2b) yielded a voxel depth of about 1500 nm and a width of about 50 μm . The vertical sides of the

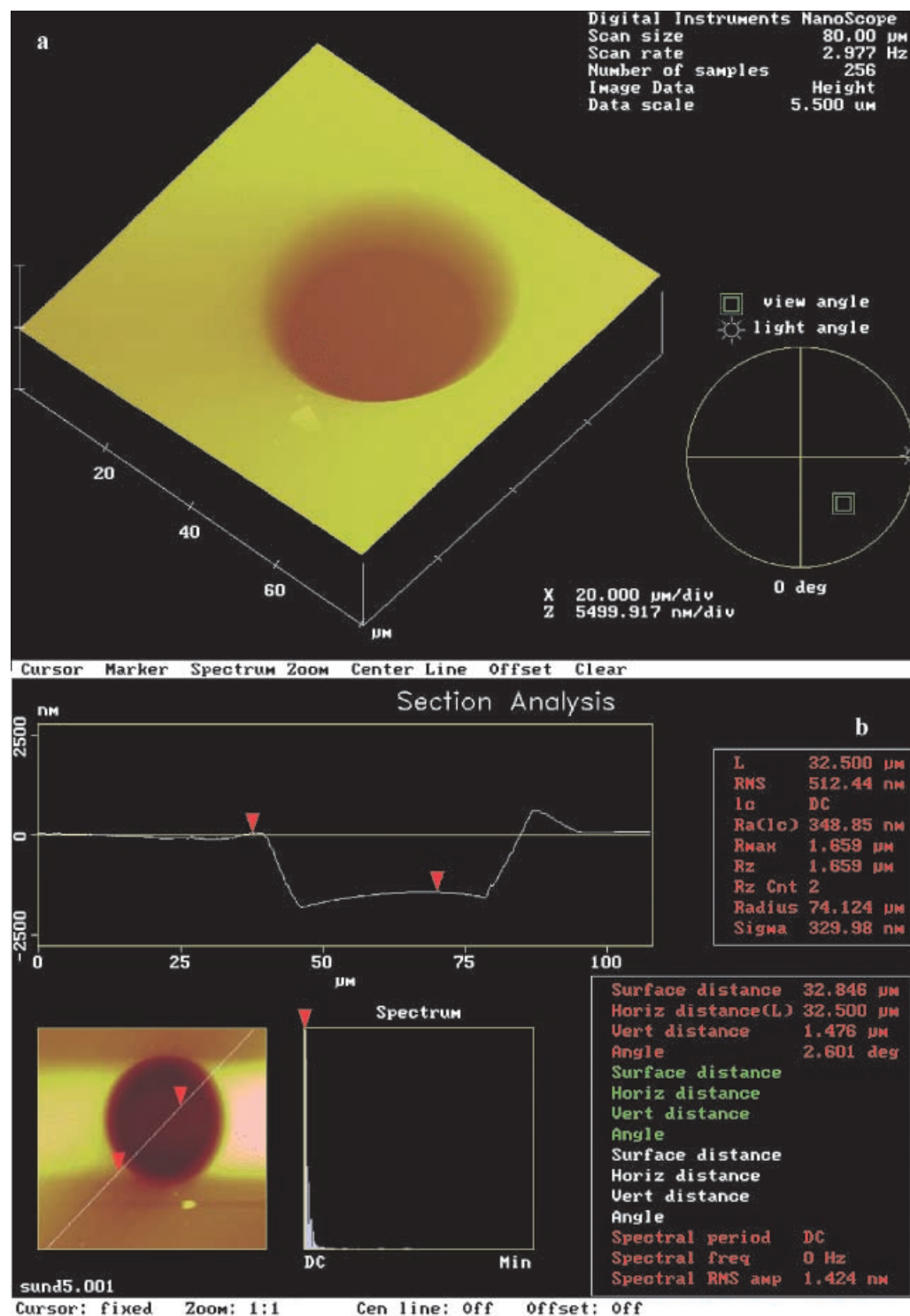


FIGURE 2 AFM images of the isometric view (a) and the plan view (b) of a voxel. Sectional analysis along the diagonal white reference line is shown in b

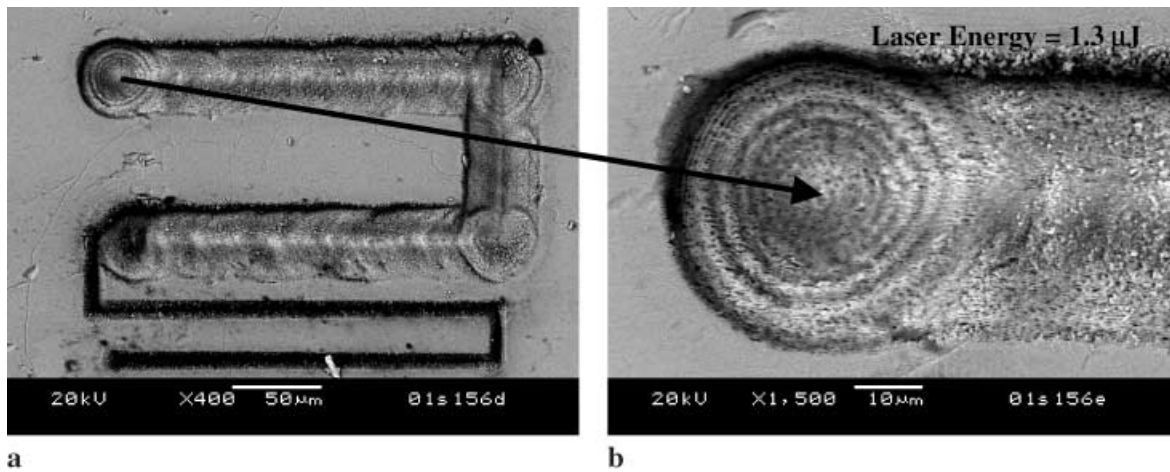


FIGURE 3 SEM of multiple-shot microexplosions in baseline glass: **a** start and end of the line written; and **b** enlarged image of the starting point shown by the arrow

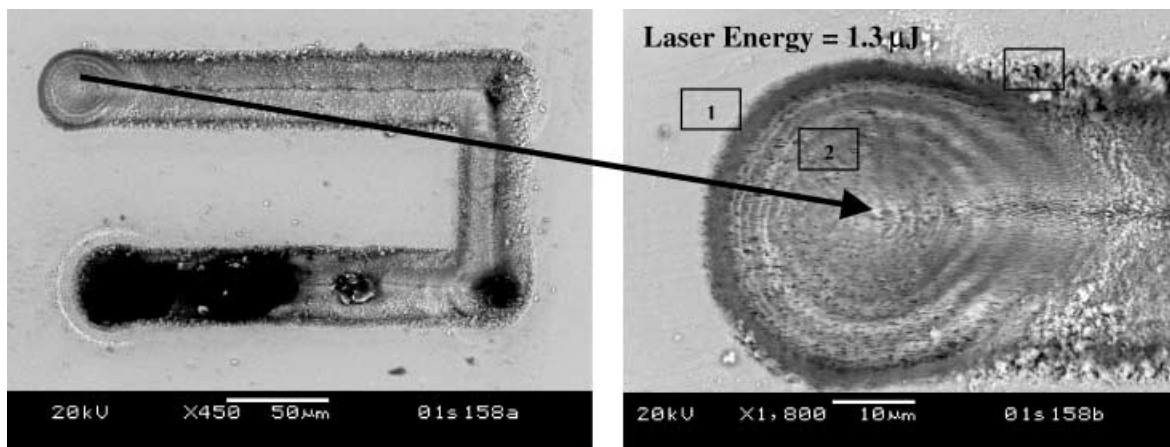


FIGURE 4 SEM images of multiple-shot microexplosions in Al_2O_3 -doped sodium tellurite glass: **a** start and end of the line written; and **b** enlarged image of the starting point shown by the arrow

sectional image are somewhat distorted due to the pyramidal geometry of the SiN AFM probe tip.

Figure 3a shows the multiple-shots structure generated by writing lines in the baseline glass. The laser beam was translated at a speed of $10 \mu\text{m/s}$ while continuously irradiating with $1.3\text{-}\mu\text{J}$ laser pulses arriving at a 1 kHz repetition rate. The concentric lines at the starting point (shown in Fig. 3b) depict the microexplosion that was initiated. EDS data collected at several places at the starting point and along the line of writing did not show any significant change in glass chemistry.

3.2 Al_2O_3 -doped glass composition

Figure 4a shows the multiple-shots structure generated when writing lines at $10 \mu\text{m/s}$ with a 1-kHz train of $1.3\text{-}\mu\text{J}$ pulses in the Al_2O_3 -doped glass. Dark regions (Fig. 4a) are discontinuities in the material, due to compaction of glass by the impact and shock waves. These regions also indicate the fluctuations in laser power during writing. EDS data collected at three different points (shown in Fig. 3b) are summarized in Table 1. The No. 2 spot inside the microexplosion region showed no detectable Al, while spot No. 3 at the edge of the region showed slight depletion of Al and Na., as compared with spot No. 1 in the bulk glass close to the region.

The data indicated a chemical gradient within the region of the microexplosions.

Element	Weight %		
	1	2	3
O K	27.38	24.38	18.09
Na K	2.07	2.24	1.44
Al K	0.33	–	0.19
Te L	70.22	73.38	80.28
Total	100.00	100.00	100.00

TABLE 1 EDS data of multiple-shot microexplosions in Al_2O_3 -doped glass. Locations of regions 1, 2, and 3 are indicated in Fig. 4b

3.3 La_2O_3 -doped glass composition

Figure 5a shows the multiple-shots structure generated when writing lines at $10 \mu\text{m/s}$ with a 1-kHz train of $1.3\text{-}\mu\text{J}$ pulses in the La_2O_3 -doped glass. The external ring fingerprinted the shock wave generated during the microexplosion. Material has been removed at the center of the region, at the start of the microexplosion, as well as along the center of the line written. The impact of the beam has created

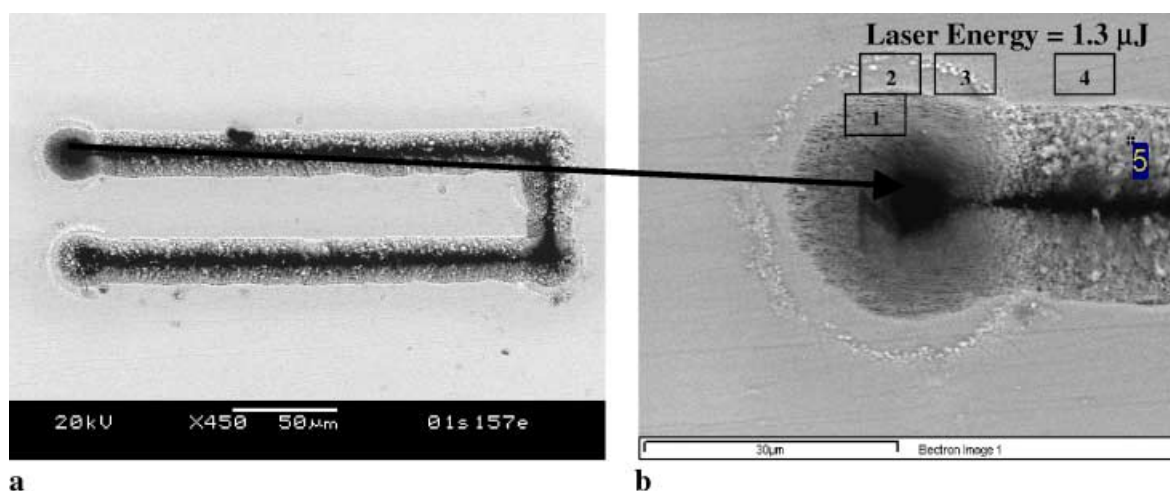


FIGURE 5 SEM images of multiple-shot microexplosions in La_2O_3 -doped sodium tellurite glass: **a** start and end of the line written; and **b** enlarged image of the starting point shown by the arrow

Element	Weight %				
	1	2	3	4	5
OK	30.01	26.40	21.13	25.59	26.88
Na K	4.17	2.37	1.69	2.41	2.52
Te L	65.82	67.27	73.52	67.76	67.12
La L	–	3.96	3.66	4.24	3.48
Total	100.00	100.00	100.00	100.00	100.00

TABLE 2 EDS data of multiple-shot microexplosions in La_2O_3 -doped glass. Locations of regions 1–5 are indicated in Fig. 5b

a crater-like feature, forcing away the material at the center (dark region at the center in Fig. 5b).

EDS data collected at five points are summarized in Table 2. The No. 1 spot inside the microexplosion region close to the center of the region showed no detectable La, while the spot Nos. 2–5 around the region of microexplosion showed slight depletion of Na and varying La concentrations. As in the case of Al_2O_3 -doped glass, the data indicated a chemical gradient within the region of the microexplosions.

Chemical gradients observed in the case of the doped (Al_2O_3 or La_2O_3) glasses (summarized in Tables 1 and 2) indicate the dopant concentration is low at the center of the microexplosion. The concentration gradually increases radially from the center to the edge of the irradiated region and reaches a maximum value in the bulk glass region. Diffusion of the dopant from the center to the edges of the microexplosions is not plausible as the laser interacts with the glass for a short time (about $1 \mu\text{s}$). One possible explanation is as follows: The impact of the laser shots drives away different species from the center of the microexplosion. Once the laser irradiation is stopped, the species driven away do not have the necessary time or energy to redistribute or diffuse back.

3.4 Micro-Raman data

Figure 6a–c shows the micro-Raman spectra of the baseline, Al_2O_3 -doped, and La_2O_3 -doped sodium tellurite glasses, respectively. The spectra compare the bulk and microexplosion spot region for each glass. The qualitative comparison of spectra compared well with the reported data in

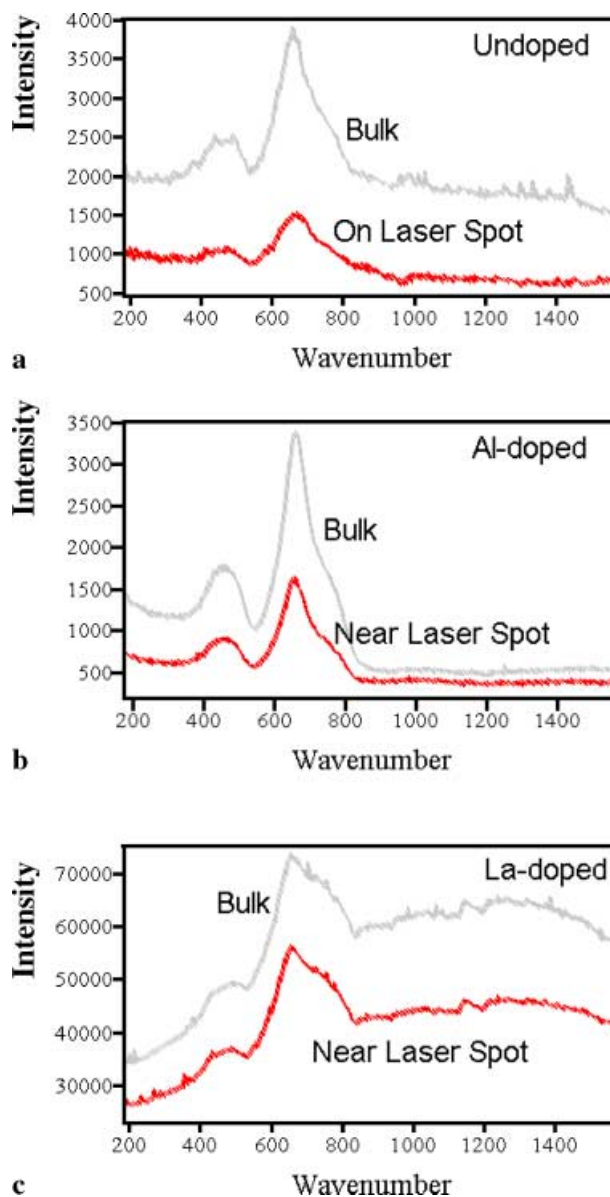


FIGURE 6 Micro-Raman data for baseline (a), Al_2O_3 -doped (b) and La_2O_3 -doped (c) glasses

the literature [34, 35]. The regions examined were single-shot regions in the case of the base glass and multiple-shot regions for doped glasses described in sections 3.1, 3.2 and 3.3, respectively. No difference in the spectra between the bulk and microexplosion regions was observed. The beam interrogated about a 10- μm spot size, thus including some dilution effect from the bulk.

4 Conclusions

This paper demonstrates microexplosions and the writing of simple structures in the near-surface region of base-line and doped (Al_2O_3 or La_2O_3) sodium tellurite glasses, using tightly focused femtosecond laser pulses. Imaging and spectrometry data showed a chemistry gradient from the center of the voxel or channel to the edge of the microexplosion or written regions, due to diffusion driven by the thermal gradient generated. However, no structural changes were observed when comparing the bulk regions with the microexplosion and laser-written regions.

ACKNOWLEDGEMENTS We wish to thank C. Windisch (PNNL) for help with the Raman experiment and R. Williford (PNNL) for help with AFM measurements. S.K. Sundaram wishes to thank the Environmental Management Science Program (EMSP) for support. Pacific Northwest National Laboratory is operated by Battelle Memorial Institute for the U.S. Department of Energy under Contract No. DE-AC06-76RL01830.

REFERENCES

- 1 J. Stanworth: *J. Soc. Glass Tech.* **36**, 217 T (1952)
- 2 A. Westman, J. Grawther: *J. Am. Ceram. Soc.* **37**, 420 (1954)
- 3 J.S. Wang, E.M. Vogel, E. Snitzer: *Opt. Mater.* **3**, 187 (1994)
- 4 S.H. Kim, T. Yoko, S. Sakka: *J. Am. Ceram. Soc.* **76**, 2486 (1993)
- 5 R. El-Mallawany: *Mater. Chem. Phys.* **53**, 93 (1998)
- 6 R. El-Mallawany: *Mater. Chem. Phys.* **60**, 103 (1999)
- 7 R. El-Mallawany: *Mater. Chem. Phys.* **63**, 109 (2000)
- 8 J. Heo, D. Lam, G.H. Sigel Jr., E.A. Mendoza, D.A. Hensley: *J. Am. Ceram. Soc.* **75**, 277 (1992)
- 9 M. Zhang, S. Mancini, W. Bresser, P. Boolchand: *J. Non-Cryst. Solids* **151**, 149 (1992)
- 10 R. El-Mallawany: *J. Appl. Phys.* **72**, 1774 (1992)
- 11 S. Neov, V. Kozhukharov, I. Gerasimova, K. Krezhov, B. Sidzhimov: *J. Appl. Phys. C* **12**, 2475 (1979)
- 12 K. Suzuki: *J. Non-Cryst. Solids* **95–96**, 15 (1987)
- 13 T. Sekiya, N. Mochida, A. Ohtsuka, M. Tonokawa: *J. Non-Cryst. Solids* **144**, 128 (1992)
- 14 M. Tatsumisago, S.K. Lee, T. Minami, Y. Kowada: *J. Non-Cryst. Solids* **177**, 154 (1994)
- 15 S. Sakida, S. Hayakawa, T. Yoko: *J. Non-Cryst. Solids* **243**, 13 (1994)
- 16 J.C. McLaughlin, S.L. Tagg, J.W. Zwanziger, D.R. Haefner, S.D. Sastri: *J. Non-Cryst. Solids* **274**, 1 (2000)
- 17 K.M. Davis, K. Muira, N. Sugimoto, K. Hirao: *Opt. Lett.* **21**, 1729 (1996)
- 18 E.N. Glezer, M. Milosavljevic, L. Huang, R.J. Finlay, T.H. Her, J.P. Callan, E. Mazur: *Opt. Lett.* **21**, 2023 (1996)
- 19 E.N. Glezer: *Ph.D. Thesis* (Harvard University 1996)
- 20 E.N. Glezer, C.B. Schaffer, N. Nishimura, E. Mazur: *Opt. Lett.* **22**, 1817 (1997)
- 21 E.N. Glezer, E. Mazur: *Appl. Phys. Lett.* **71**, 882 (1997)
- 22 K. Muira, J. Qiu, H. Inouye, T. Mitsuyu, K. Hirao: *Appl. Phys. Lett.* **71**, 3329 (1997)
- 23 E.N. Glezer, L. Huang, R.J. Finlay, T.H. Her, J.P. Callan, C.B. Schaffer, E. Mazur: *Proc. 28th An. Boulder Damage Symposium*, Boulder, CO, USA, SPIE, Bellingham, WA (1996)
- 24 C.B. Schaffer, E.N. Glezer, N. Nishimura, E. Mazur: *Proc. SPIE* **3269**, 36 (1998); C.B. Schaffer, N. Nishimura, E. Mazur: *Proc. SPIE* **3451**, 2 (1998)
- 25 C.B. Schaffer, A. Brodeur, N. Nishimura, E. Mazur: *Proc. SPIE* **3616**, 143 (1999)
- 26 C.B. Schaffer, A. Brodeur, E. Mazur: *Meas. Sci. Technol.* **12**, 1784 (2001)
- 27 C.B. Schaffer, A. Brodeur, J.F. Garcia, E. Mazur: *Opt. Lett.* **26**, 93 (2001)
- 28 C.B. Schaffer: *Ph.D. Thesis* (Harvard University, 2001)
- 29 D. Homelle, S. Wielandy, A.L. Gaeta, N.F. Borrelli, C. Smith: *Opt. Lett.* **24**, 1311 (1999)
- 30 A.M. Streltsov, N.F. Borrelli: *Opt. Lett.* **26**, 42 (2001)
- 31 L. Sudrie, M. Franco, B. Prade, A. Mysyrewicz: *Opt. Commun.* **171**, 279 (1999)
- 32 J.W. Chan, T.R. Huser, S. Risbud, D.M. Krol: *Opt. Lett.* **26**, 1726 (2001)
- 33 B.K.A. Ngoi, K. Venkatakrishnan, E.N.L. Lim, B. Tan, L.H.K. Koh: *Opt. Lasers Eng.* **35**, 361 (2001)
- 34 T. Sekiya, N. Mochida, A. Soejima: *J. Non-Cryst. Solids* **191**, 115 (1995)
- 35 H. Li, Y. Su, S.K. Sundaram: *J. Non-Cryst. Solids* **293–295**, 402 (2001)